The Astrophysical Journal, 601:644–653, 2004 February 1

NEAR-INFRARED COLORS OF GAMMA-RAY BURST AFTERGLOWS AND COSMIC REIONIZATION HISTORY

Akio K. Inoue,[1] Ryo Yamazaki,[1] and Takashi Nakamura
Department of Physics, Kyoto University, Kyoto 606-8502, Japan;
akinoue@tap.scphys.kyoto-u.ac.jp, yamazaki@tap.scphys.kyoto-u.ac.jp, takashi@tap.scphys.kyoto-u.ac.jp
Received 2003 August 11; accepted 2003 October 13

ABSTRACT

We discuss a way to study the cosmic reionization history using near-infrared (NIR) observations of the afterglows of high-redshift ($5 \lesssim z \lesssim 25$) gamma-ray bursts (GRBs) that will be detected by the *Swift* satellite. In principle, details of the cosmic reionization history should be imprinted in the NIR spectra of GRB afterglows. However, spectroscopy with a space telescope is required to obtain such information for very high redshifts ($z \gtrsim 15$) unless the neutral fraction of the high-z universe is less than 10^{-6}. The broadband photometry has higher sensitivity than the spectroscopy, so that NIR photometric follow-up of GRB afterglows is very promising for examining cosmic reionization history. A few minutes exposure with a 8 m class ground-based telescope of the afterglows of the high-z GRBs will reveal how many times reionization occurred in the universe.

Subject headings: cosmology: observations — gamma rays: bursts — intergalactic medium — radiative transfer — techniques: photometric

1. INTRODUCTION

The evolutionary study of the intergalactic medium (IGM) is now one of the most active fields in astrophysics. In particular, the cosmic reionization history of the IGM has attracted many researchers in recent years (see Loeb & Barkana 2001 for a review). The Gunn-Peterson trough shortward of the Lyα resonance (Gunn & Peterson 1965) in the spectrum of quasars with redshift $z \sim 6$ indicates that the end of the reionization epoch is $z \sim 6$ (Becker et al. 2001; White et al. 2003). On the other hand, the recent observation of the polarization of the cosmic microwave background (CMB) by *WMAP* suggests that the beginning of reionization is $z \sim 20$ (Spergel et al. 2003; Kogut et al. 2003). One might think that there is a discrepancy between the two observations.

The detailed simulation of the six-dimensional radiative transfer shows that the reionization process proceeds slowly in an inhomogeneous universe (e.g., Nakamoto, Umemura, & Susa 2001). If the reionization began at $z \sim 20$, the neutral fraction in the universe decreased gradually, and the universe was ionized almost completely at $z \sim 6$, the apparent discrepancy can be resolved (Wyithe & Loeb 2003a; Haiman & Holder 2003; Ciardi, Ferrara, & White 2003; Chiu, Fan, & Ostriker 2003; Sokasian et al. 2003; Onken & Miralda-Escudé 2003). The scenario that the initial, partially ionized epoch was followed by complete ionization can explain the large Thomson scattering opacity observed from the CMB polarization and is also consistent with the previous picture in which the end of reionization is $z \sim 6$.

Cen (2003a, 2003b) and Wyithe & Loeb (2003b) recently proposed a new reionization scenario: the universe was reionized twice. Even in an inhomogeneous universe, enough strong ultraviolet (UV) background radiation can ionize the universe quickly. At $z \sim 20$, the first reionization was made by Population III stars (metal-free stars) with a top-heavy initial mass function (IMF), which yields a much higher UV emissivity than those of normal Population I and II stars. Then, the universe was partially recombined at $z \sim 15$ when the transition from Population III to II occurred and the UV emissivity was suddenly suppressed by the different IMF. Finally, the number of UV photons from Population II stars increased gradually, ionizing the universe again at $z \sim 6$.

Cen's scenario can also resolve the discrepancy, but it is different from others in the history of cosmic reionization; the first complete ionization was followed by the partially ionized epoch and then by the second complete ionization. We should assess whether Cen's scenario is favored by other observations. In this paper, an assessment that uses afterglows of gamma-ray bursts (GRBs) is discussed.

The usefulness of GRBs to investigate the high-z universe has been pointed out by many authors (e.g., Lamb & Reichart 2000; Ciardi & Loeb 2000; Barkana & Loeb 2004). It has been strongly suggested that the long-duration GRBs arise from the collapse of a massive star (Galama et al. 1998; Uemura et al. 2003; Hjorth et al. 2003; Price et al. 2003; Stanek et al. 2003; Matheson et al. 2003). Hence, GRBs can occur at very high z once massive stars are formed. For example, the *Swift* satellite[2] is expected to detect $\sim$10 GRBs per year occurring at $z \gtrsim 10$ (Lamb & Reichart 2000). Furthermore, if we fix an observing time from the prompt emission, the observed afterglow flux does not become so faint even for extremely high z GRBs because the earlier phase of the afterglow is observed in the cosmological rest frame (Ciardi & Loeb 2000).

In this paper, we show that near-infrared (NIR) photometric follow-ups of GRB afterglows are very useful to investigate how many times cosmic reionization occurred. Although many techniques to probe the reionization history have been proposed so far, e.g., hydrogen 21 cm line tomography (Madau, Meiksin, & Rees 1997; Carilli, Gnedin, & Owen 2002; Furlanetto & Loeb 2002), Lyα damping wing measurements (Miralda-Escudé 1998; Barkana & Loeb 2004),

[1] Research Fellow of Japan Society for the Promotion of Science.

[2] See http://swift.gsfc.nasa.gov/.

metal absorption lines (Oh 2002; Furlanetto & Loeb 2003), CMB polarization anisotropy (Haiman & Holder 2003), and dispersion measures in GRB radio afterglows (Ioka 2003; Inoue 2003), NIR photometric colors may be the most promising technique using *current* facilities.

In order to investigate the reionization history using our photometric method, we need to determine redshifts of GRBs by other means, e.g., detections of iron lines in X-ray afterglow spectra (Mészáros & Rees 2003) and of the Lyα break in NIR spectra, or empirical methods by using only the γ-ray data (Fenimore & Ramirez-Ruiz 2000; Norris, Marani, & Bonnell 2000; Ioka & Nakamura 2001; Amati et al. 2002; Atteia 2003; Murakami et al. 2003; Yonetoku et al. 2003). Even if redshifts of GRBs are unknown prior to follow-up observations, it is worth performing NIR photometry as early as possible, since $\sim$10% of GRBs are expected to be located at $z \gtrsim 10$ (Bromm & Loeb 2002). In practice, such follow-up observations of every GRB are possible. Even after early NIR follow-up, we will be able to determine the redshifts. In this paper, we show that near-infrared (NIR) photometric follow-ups of GRB afterglows provide significantly important information on the cosmic reionization history.

The structure of this paper is as follows: we start from a brief summary of the IGM opacity fromneutral hydrogen in § 2. In § 3, the possible scenario of a very low neutral fraction at very high-z is discussed. Then, we examine the NIR spectra and colors of GRB afterglows in §§ 4 and 5, respectively. Finally, we discuss a way to obtain the cosmic reionization history and the advantages and disadvantages of our method in § 6.

We adopt the standard set of the ΛCDM cosmology throughout the paper: $H_0 = 70$ km s^{-1} Mpc^{-1}, $\Omega_M = 0.3$, $\Omega_\Lambda = 0.7$, and $\Omega_b = 0.04$.

2. IGM OPACITY

Suppose an observer at $z = 0$ observes a source with $z = z_S$ at the observer's frequency ν_0. The radiation from the source is absorbed by the Lyman series lines and the photoionization of the intervening neutral hydrogen (Gunn & Peterson 1965). The hydrogen cross section at the rest frame frequency ν is

$$\sigma_{\rm H\,I}(\nu) = \sigma_{\rm LC}(\nu) + \sum_i \sigma_i(\nu), \tag{1}$$

where $\sigma_{\rm LC}(\nu)$ is the cross section for the Lyman continuum photons ($h\nu \geq 13.6$ eV) and $\sigma_i(\nu)$ is the cross section for the ith line of the Lyman series, i.e., $i = {\rm Ly}\alpha$, Lyβ, Lyγ, etc. Here we consider lines up to $i = 40$. The optical depth for the observer's frequency ν_0 is given by

$$\tau_{\nu_0}(z_S) = \tau^{\rm LC}_{\nu_0}(z_S) + \sum_i \tau^i_{\nu_0}(z_S), \tag{2}$$

$$\tau^{\rm LC}_{\nu_0}(z_S) = \int_0^{z_S} \sigma_{\rm LC}[\nu_0(1+z)] n_{\rm H\,I}(z) \frac{c\,dz}{(1+z)H(z)}, \tag{3}$$

and

$$\tau^i_{\nu_0}(z_S) = \int_0^{z_S} \sigma_i[\nu_0(1+z)] n_{\rm H\,I}(z) \frac{c\,dz}{(1+z)H(z)}, \tag{4}$$

where $n_{\rm H\,I}(z)$ is the number density of neutral hydrogen at redshift z, $H(z)$ is the Hubble constant at redshift z, and c is the speed of light.

The cross section for the Lyman continuum photons is given by $\sigma_{\rm LC}(\nu) = \sigma_{\rm L}(\nu/\nu_{\rm L})^{-3}$, where $\sigma_{\rm L} = 6.30 \times 10^{-18}$ cm^2 and the Lyman limit frequency $\nu_{\rm L} = 3.29 \times 10^{15}$ Hz (Osterbrock 1989). Thus, we obtain

$$\tau^{\rm LC}_{\nu_0}(z_S) = \sigma_{\rm L}\left(\frac{\nu_{\rm L}}{\nu_0}\right)^3 n_{\rm H,0} c \int_{z_{\rm min}}^{z_S} \frac{x_{\rm H\,I}(z)\,dz}{(1+z)H(z)}, \tag{5}$$

where $x_{\rm H\,I}(z)$ is the neutral fraction at redshift z and $z_{\rm min} = \max[0, (\nu_{\rm L}/\nu_0) - 1]$. The neutral fraction $x_{\rm H\,I}(z)$ is defined as $n_{\rm H\,I}(z)/n_{\rm H}(z)$, where $n_{\rm H}(z) = n_{\rm H,0}(1+z)^3$ is the cosmic mean number density of hydrogen atoms at redshift z, with $n_{\rm H,0}$ being the present density. The effect of the inhomogeneity of the universe can be expressed in the definition of $x_{\rm H\,I}$ (see § 3 below). Since we need the condition $z_{\rm min} < z_S$ to integrate equation (5), $\tau^{\rm LC}_{\nu_0}(z_S) = 0$ when $\nu_0 \leq \nu_{\rm L}/(1+z_S)$.

The line cross section $\sigma_i(\nu)$ has a very sharp peak at the line center frequency. The width is well characterized by the Doppler width, $\Delta\nu_{\rm D}$. That is, $\sigma_i(\nu) \simeq \sigma_i$ for $|\nu - \nu_i| \leq \Delta\nu_{\rm D}$, and $\sigma_i(\nu) \simeq 0$ for $|\nu - \nu_i| > \Delta\nu_{\rm D}$, where σ_i and ν_i are the cross section and the frequency of the ith line center, respectively. Since $\nu = \nu_0(1+z)$, we integrate the right hand side of equation (4) over a narrow redshift width of $\Delta(1+z) = 2(\Delta\nu_{\rm D}/\nu_i)(1+z_i)$ around $1 + z_i = \nu_i/\nu_0$. Therefore, we obtain

$$\tau^i_{\nu_0}(z_S) \simeq 2\left(\frac{\sqrt{\pi}e^2 f_i}{m_e c \nu_i}\right)\left[\frac{c n_{\rm H\,I}(z_i)}{H(z_i)}\right], \tag{6}$$

where we have substituted $\sigma_i = \sqrt{\pi}e^2 f_i/(m_e c \Delta\nu_{\rm D})$, in which e is the electric charge, f_i is the absorption oscillator strength of the ith line, and m_e is the electron mass. The values of f_i and ν_i are taken from Wiese, Smith, & Glennon (1966). This time we are also restricted by $z_i \leq z_S$. Thus, the above equation is valid only when $\nu_0 \geq \nu_i/(1+z_S)$; otherwise $\tau^i_{\nu_0}(z_S) = 0$.

For the Lyα line, the opacity becomes

$$\tau_{{\rm Ly}\alpha} \simeq 2.6 \times 10^6 x_{\rm H\,I}(z)\left(\frac{1+z}{20}\right)^{3/2}, \tag{7}$$

where we approximate $H(z) \approx H_0 \Omega_M^{1/2}(1+z)^{3/2}$ and adopt $n_{\rm H\,I}(z) = x_{\rm H\,I}(z) n_{\rm H,0}(1+z)^3$. This is the Gunn-Peterson optical depth (Gunn & Peterson 1965; Peebles 1993). From this equation, if $x_{\rm H\,I} \gtrsim 10^{-6}$, the IGM is opaque for photons bluer than the source Lyα line. Conversely, we can estimate $x_{\rm H\,I}$ if $\tau^{{\rm Ly}\alpha}$ is determined observationally (e.g., Becker et al. 2001; White et al. 2003).

3. NEUTRAL FRACTION AND STAR FORMATION RATE

In the following sections, we assume a neutral hydrogen fraction, $x_{\rm H\,I} \sim 10^{-6}$ at $z \sim 20$ for calculations of spectra and colors of GRB afterglows. Before such calculations, we show that $x_{\rm H\,I} \sim 10^{-6}$ is possible in a very high z universe.[3]

In general, the neutral fraction, $x_{\rm H\,I}(z)$ is spatially variable. However, we discuss only its mean value for simplicity. The averaged $x_{\rm H\,I}$ is determined by the UV intensity of the background radiation and the inhomogeneity of the hydrogen

[3] In Fig. 9 of Cen (2003a), the neutral fraction decreases up to 10^{-4}. However, it is an artificial limit in his calculation (Cen 2003, private communication).

number density at redshift z. Even at very high z, the recombination timescale is much less than the Hubble timescale. Thus, we assume ionization equilibrium. In that case, the mean neutral fraction for a highly ionized medium (i.e., $x_{\rm H\,I} \ll 1$) is given by $x_{\rm H\,I} \approx Cn_{\rm H}\alpha/\Gamma_{\rm H\,I}$, where $C = \langle n_{\rm H}^2\rangle/\langle n_{\rm H}\rangle^2$ is the clumping factor, $n_{\rm H}$ is the number density of hydrogen nuclei, α is the recombination coefficient, and $\Gamma_{\rm H\,I} = \int \sigma_{\rm LC}(\nu)cn_\nu\, d\nu$ is the H I photoionization rate, where n_ν is the photon number density per frequency. Therefore, the UV background intensity is required to estimate $x_{\rm H\,I}$ even if we know the clumping factor from the model of cosmological structure formation.

How many photons are required to limit the neutral hydrogen fraction to a very low level? Approximately, the H I photoionization rate is estimated to be $\Gamma_{\rm H\,I} \sim \sigma_{\rm L}cn_{\rm ion}$, with $n_{\rm ion}$ being the number density of ionizing photons. Hence, we find

$$\frac{n_{\rm ion}}{n_{\rm H}} \sim \frac{C\alpha}{\sigma_{\rm L}cx_{\rm H\,I}} \sim C\left(\frac{10^{-6}}{x_{\rm H\,I}}\right), \tag{8}$$

where the case B recombination rate $\alpha = 2.73 \times 10^{-13}$ cm^3 s^{-1} is adopted (Osterbrock 1989). Now, we are interested in a very high redshift universe ($z \sim 20$) where the clumping factor is on the order of unity. Therefore, we find that only one photon per hydrogen nuclei is sufficient to keep $x_{\rm H\,I} \sim 10^{-6}$.

Then, we examine how many stars are required to maintain the photon density. Since a proton recombines with an electron on a certain timescale, a continuous supply of ionizing photons is needed to keep $n_{\rm ion} \sim n_{\rm H}$. Since the recombination timescale is $\sim 1/n_{\rm H}\alpha$ for $x_{\rm H\,I} \ll 1$, the required photon emissivity per unit volume is estimated to be $\epsilon_{\rm ion} \sim n_{\rm ion}n_{\rm H}\alpha \sim Cn_{\rm H}^2\alpha^2/x_{\rm H\,I}\sigma_{\rm L}c$. On the other hand, the emissivity is given by $\epsilon_{\rm ion} = f_{\rm esc}\epsilon_{\rm LC}\rho_{\rm SFR}(1+z)^3$, where $f_{\rm esc}$ is the escape fraction of Lyman continuum from primordial galaxies, $\epsilon_{\rm LC}$ is the Lyman continuum photon emissivity per unit stellar mass, and $\rho_{\rm SFR}$ is the star formation density per unit time per unit comoving volume. Therefore, the required star formation density is

$$\frac{\rho_{\rm SFR}}{M_\odot\ {\rm yr}^{-1}\ {\rm Mpc}^{-3}} \sim 0.1C\left(\frac{0.1}{f_{\rm esc}}\right)\left(\frac{10^{61}\ {\rm photons}\ M_\odot^{-1}}{\epsilon_{\rm LC}}\right) \times \left(\frac{10^{-6}}{x_{\rm H\,I}}\right)\left(\frac{1+z}{20}\right)^3. \tag{9}$$

Although the photon emissivity at high z is very uncertain because we do not know the stellar mass distribution, we estimate the emissivity using the Starburst 99 model (Leitherer et al. 1999)[4] and assuming a Salpeter mass function with various mass ranges. The estimated values of $\epsilon_{\rm LC}$ are summarized in Table 1. Continuous star formation lasting longer than several Myr is assumed in the calculation. The Population III stars are likely to have a top-heavy mass function (e.g., Nakamura & Umemura 2001). Hence, the case of 10–100 $M_\odot$ in Table 1 may be suitable. In this case, the required star formation density to maintain $x_{\rm H\,I} \sim 10^{-6}$ is $\sim 0.05\ M_\odot\ {\rm yr}^{-1}\ {\rm Mpc}^{-3}$ (comoving) when $f_{\rm esc} = 0.1$ and $C = 1$.

Is this star formation density possible? The latest observations suggest that the star formation density retains a level of $\sim 0.1\ M_\odot\ {\rm yr}^{-1}\ {\rm Mpc}^{-3}$ from $z \sim 1$ to $z \sim 6$ (Giavalisco et al. 2003). Such a level of star formation may continue toward higher z. Moreover, a semianalytic model shows 0.01–0.1 $M_\odot\ {\rm yr}^{-1}\ {\rm Mpc}^{-3}$ at $z \sim 20$, depending on the assumed star formation efficiency (Somerville & Livio 2003). Thus, we can expect $\sim 0.05\ M_\odot\ {\rm yr}^{-1}\ {\rm Mpc}^{-3}$, and that, $x_{\rm H\,I} \sim 10^{-6}$ at $z \sim 20$. In addition, we note that the escape fraction may be much larger than 0.1 assumed above if Population III stars are formed in low-mass halos.

[4] See http://www.stsci.edu/science/starburst99/.

4. NEAR-INFRARED SPECTRA

Let us discuss the observed spectra of GRB afterglows in the NIR bands. To do so, an afterglow spectral model is required. We adopt a simple afterglow model: synchrotron radiation from a relativistic shock (Sari, Piran, & Narayan 1998). More specifically, we adopt equations (1)–(5) in Ciardi & Loeb (2000) who take into account the effect of the cosmological redshift. The adopted parameters are a magnetic energy fraction of $\epsilon_B = 0.1$, an electron energy fraction of $\epsilon_e = 0.2$, a spherical shock energy of $E = 10^{52}$ ergs, an ambient gas number density of $n = 10$ cm^{-3}, and a power-law index of the electron energy distribution $p = 2.5$.

First, we consider the observed afterglow spectra in a hypothetical, perfectly neutral universe for comparison. In Figure 1, we show the expected afterglow spectra in the neutral universe observed 1 hr after the burst in the observer's frame. Because of Lyα line absorption, the continuum bluer than the Lyα line in the source frame (the observed wavelength $0.1216[1+z_S]$ μm) is completely damped. Thus, we can find the Lyα break clearly. From the observed wavelength of the Lyα break, we can determine the redshift of the GRB. If we observe the afterglow through a filter, radiation from a source with a redshift higher than the characteristic redshift of the filter cannot be detected because of the Lyα break. For example, the effect starts from $z_S \simeq 8$ for the J band and a source with $z_S \gtrsim 11$ cannot be seen through the filter, i.e., *J dropout*. These characteristic redshifts are summarized in Table 2. However, we have a chance to see the source beyond the dropout redshift if the universe is highly ionized, as we show later.

Next, we examine what is observed if the very high z universe is ionized completely as proposed by Cen (2003a, 2003b). Let us set the neutral fraction, $x_{\rm H\,I}$, of the universe in the redshift range $15 \le z < 20$ to be very small and $x_{\rm H\,I} \sim 1$ for $z < 15$ and $z \ge 20$. That is, we assume that Population III stars ionized the universe at $z = 20$ and the sudden change of the IMF due to the transition from Population III to II occurred at $z = 15$. The neutral fraction is determined by the background UV intensity produced by Population III stars. However, the intensity is quite uncertain, so we choose two cases, $x_{\rm H\,I} = 10^{-6}$ and 10^{-7} (see also Fig. 5 in § 6). We present a way to constrain $x_{\rm H\,I}$ from the observations later.

TABLE 1

STAR FORMATION DENSITY REQUIRED TO MAINTAIN $x_{\rm H\,I} \sim 10^{-6}$ AT $z \sim 20$

Stellar Mass Range ($M_\odot$)	$\epsilon_{\rm LC}$ (10^{61} photons $M_\odot^{-1}$)	$\rho_{\rm SFR}$ ($M_\odot\ {\rm yr}^{-1}\ {\rm Mpc}^{-3}$)
10–100	2	0.05
1–100	0.7	0.1
0.1–100	0.3	0.3

NOTE.—We calculate the Lyman continuum photon emissivity per unit stellar mass, $\epsilon_{\rm LC}$, from the Starburst 99 model (Leitherer et al. 1999) by assuming the Salpeter initial mass function with the tabulated mass range. We also assume the escape fraction $f_{\rm esc} = 0.1$ and the clumping factor $C = 1$ in calculating the star formation density.

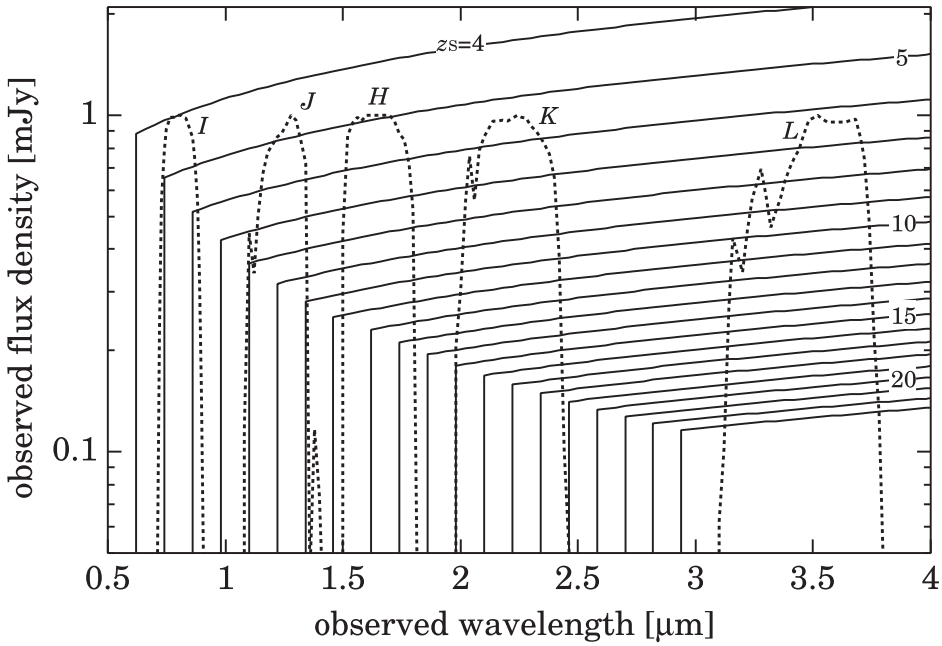

FIG. 1.—Afterglow spectra in the hypothetical neutral universe. *Solid curves*: Afterglow spectra of gamma-ray bursts at redshift $z_S = 4$–23. The observing time is set to be 1 hr after the burst for all curves. *Dotted curves*: Filter transmissions of *I*, *J*, *H*, *K*, and *L* bands (Bessell & Brett 1988; Bessell 1990). These transmission curves are scale-free.

In Figure 2, we show the expected spectra of the GRB afterglow. The solid, short-dashed, long-dashed, dot-dashed, and dotted curves are the expected afterglow spectra of the GRB at $z_S = 22$, 20, 18, 15, and 13, respectively. The observing time is assumed to be 1 hr after the prompt emission in the observer's frame. We find the clear Lyα breaks in the spectra. Since $x_{\rm H\,I} = 10^{-6}$ at $15 \le z < 20$ is assumed in Figure 2*a* (or 10^{-7} at Fig. 2*b*), the IGM opacity is of order of unity (or 0.1 for Fig. 2*b*) in that redshift range (see eq. [7]). Thus, the continuum bluer than the Lyα break of GRBs with $z_S > 15$ still remains of order of 10 μJy (or 100 μJy) in $\sim$2–2.5 μm, i.e., in the *K* band (see the thin solid curve indicated as *K*; we adopt the filter system of Bessell & Brett 1988). The spectral break at $\lambda = 1.94$ [$= 0.1216(1+15)$ μm] is due to the neutral hydrogen below $z = 15$. Thus, the continuum blueward of the break wavelength in the observer's frame from the $z_S \ge 15$ source is completely extinguished. The spectra of the sources with $z_S < 15$ are the same as those shown in Figure 1. For the $z_S = 22$ case, the spectrum shows the second break at $\lambda = 2.36$ [$= 0.1026(1+22)$ μm]. This is the Lyβ break due to neutral hydrogen near the GRB. Here we have assumed $x_{\rm H\,I} \sim 1$ for $z \ge 20$.

The structure corresponding to the reionization history appears in the spectra of the GRB afterglows shown in Figure 2 (see also Haiman & Loeb 1999). If we could detect the continuum rising at $\lambda = 2.55$ [$= 0.1216(1+20)$ μm] in the spectrum of a GRB with $z_S = 22$, we would find the starting epoch of the first reionization as $z = 20$. On the other hand, the end of the first reionization, in other words, the transition epoch from Population III to II is seen in the spectral break at $\lambda = 1.94$ [$= 0.1216(1+15)$ μm].

The suitable band to determine the ionization history depends on the redshift of the reionization epoch. From Figure 1 (see also Table 2), we find that *I*-, *J*-, *H*-, and *K*-band spectroscopies are suitable to find the reionization epoch at $z \simeq$ 5–7, 8–11, 11–14, and 15–20, respectively. In any case, observations to detect spectral signatures in NIR afterglow spectra of GRBs are strongly encouraged. If $x_{\rm H\,I}$ is smaller than 10^{-6}, we can clearly see the difference from Figure 1 and confirm double reionization.

In the above discussion, we assumed $x_{\rm H\,I} = 10^{-6}$ and 10^{-7}. Let us argue what will happen for different values of $x_{\rm H\,I}$. If $x_{\rm H\,I} \gtrsim 10^{-6}$, the remaining flux decreases exponentially because the IGM opacity becomes much larger than unity; for example, the flux is about 1 nJy for $x_{\rm H\,I} = 6 \times 10^{-6}$ and about 1 pJy for $x_{\rm H\,I} = 10^{-5}$. It is quite difficult to detect such a low-level flux.

TABLE 2
CHARACTERISTIC REDSHIFTS OF NIR FILTERS

Filter	$z_{\rm Ly\alpha,in}$	$z_{\rm Ly\alpha,out}$
I	5.0	6.6
J	8.0	10.8
H	11.4	14.0
K	15.4	19.4
L	24.6	30.6

NOTE.—$z_{\rm Ly\alpha,in}$ and $z_{\rm Ly\alpha,out}$ are the redshifts at which the Lyα break enters and goes out of the filter transmission, respectively.

5. NEAR-INFRARED COLORS

Photometric observations are more readily available than spectroscopy. We examine the expected apparent NIR colors of GRB afterglows. Although we can discuss the apparent magnitude of the afterglows in one photometric filter, their dispersion is very large because the luminosity of the afterglows depends on many uncertain parameters such as the jet opening angle, the ambient matter density, the magnetic energy fraction, and the relativistic electron energy fraction. On the other hand, the dispersion of the apparent colors can be quite small because the color does not depend on the absolute luminosity but only on the spectral shape, which does not change significantly in the observed NIR bands.

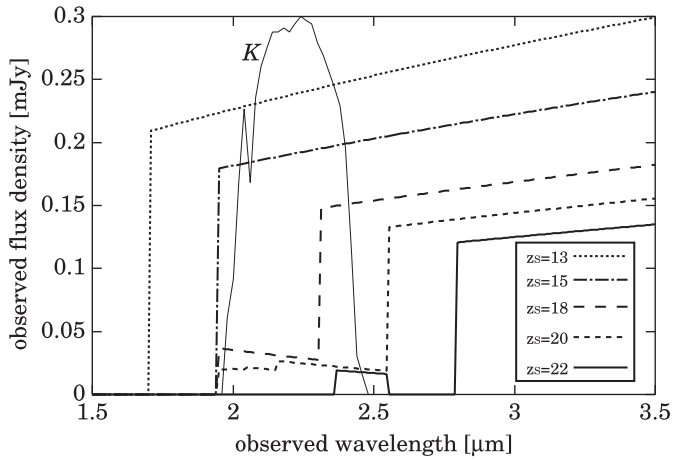

FIG. 2*a*

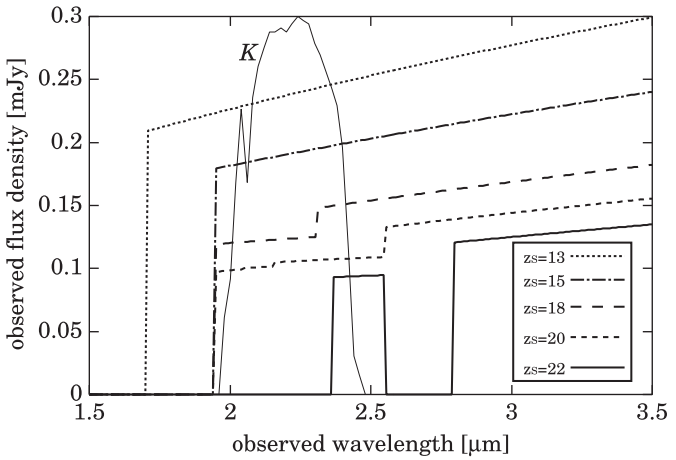

FIG. 2*b*

FIG. 2.—Expected near-infrared afterglow spectra of very high redshift gamma-ray bursts. The solid, short-dashed, long-dashed, dot-dashed, and dotted curves are the cases of source redshift $z_S = 22$, 20, 18, 15, and 13, respectively. The observing time is set to be 1 hr after the burst for all curves. The neutral fraction in $15 \leq z < 20$ is assumed to be 10^{-6} and 10^{-7} for (*a*) and (*b*), respectively. *Thin solid curve*: Filter transmission of *K* band (Bessell & Brett 1988). This transmission curve is scale-free.

The apparent magnitude[5] in a filter band denoted as i is defined by

$$m_i = -2.5 \log F_i / F_{i,0}, \tag{10}$$

where $F_{i,0}$ is the zero point flux density of the filter and F_i is the mean flux density through the filter, which is

$$F_i = \frac{\int T_{i,\nu} f_\nu e^{-\tau_\nu}\, d\nu}{\int T_{i,\nu}\, d\nu}, \tag{11}$$

where $T_{i,\nu}$ is the transmission efficiency of the filter and $f_\nu e^{-\tau_\nu}$ is the flux density entering the filter. If there is no intervening absorber between the source and the telescope, $\tau_\nu = 0$.

The observed color between two filter bands, i and j (filter i is bluer than filter j), is given by

$$m_i - m_j = (m_i - m_j)^{\rm int} + (\Delta m_i - \Delta m_j), \tag{12}$$

where $(m_i - m_j)^{\rm int}$ is the intrinsic color of the source, and Δm_i and Δm_j are the absorption amounts in the filters i and j, respectively. When we consider NIR filter bands and high-z GRBs (for example, $z = 15$), the intrinsic afterglow spectrum is predicted to be proportional to $\nu^{-1/2}$ from $\sim$1 minute to several hours after the burst occurrence and proportional to $\nu^{-p/2}$ for later times in the standard afterglow model (Sari et al. 1998; Ciardi & Loeb 2000). Other parameters adopted are described in the beginning of § 3. In Table 3, we tabulate the intrinsic colors of the sources for two cases of the spectral shape.

The absorption amount in the filter i is

$$\Delta m_i \equiv m_i - m_i^{\rm int} = -2.5 \log \frac{\int T_{i,\nu} f_\nu e^{-\tau_\nu}\, d\nu}{\int T_{i,\nu} f_\nu\, d\nu}, \tag{13}$$

where $m_i^{\rm int} = m_i(\tau_\nu = 0)$ is the intrinsic (no absorption) apparent magnitude. In a certain bandwidth $\Delta\nu$, the difference in the optical depth $\Delta\tau$ is estimated as $|\Delta\tau/\tau| = 3/2(1+z)^{-1}|\Delta(1+z)| \sim (1+z)^{-1}|\Delta\nu/\nu|$ from equation (7). Since $\Delta\nu$ of the filter transmission is smaller than the effective frequency of the filter, i.e., $\Delta\nu/\nu < 1$, and also $z \gtrsim 5$, $\Delta\tau/\tau \ll 1$, that is, the term $e^{-\tau_\nu}$ in the integral of the numerator in equation (13) can be regarded as almost constant. Hence, we obtain approximately $\Delta m_i \approx 1.086\tau_{\rm eff}$, where $\tau_{\rm eff}$ is the effective IGM opacity in the filter i.

Now we can estimate the observed color by equation (12) if Δm_i is known. Knowing Δm_i is equivalent to knowing the IGM effective opacity $\tau_{\rm eff}$, which is the opacity averaged between the redshift at which the Lyα break comes into the filter bandwidth ($z^i_{{\rm Ly}\alpha,{\rm in}}$; see Table 2) and the source redshift (z_S). The neutral hydrogen in $z < z^i_{{\rm Ly}\alpha,{\rm in}}$ cannot absorb the photons passing through the filter i. We note that the neutral hydrogen lying beyond the redshift at which the Lyα break goes out of the filter bandwidth ($z^i_{{\rm Ly}\alpha,{\rm out}}$; see Table 2) absorbs the photons through the filter i because of the higher order Lyman series lines like Lyβ, Lyγ, etc., and the photoionization process. As a result, $\tau_{\rm eff}$ is determined by the neutral fraction $x_{\rm H\,I}$ in the redshift range $z^i_{{\rm Ly}\alpha,{\rm in}} \leq z \leq z_S$. Since $x_{\rm H\,I}$ at high z is uncertain, we assume that $x_{\rm H\,I}$ is constant in the above range for simplicity. The real $x_{\rm H\,I}$ might vary significantly in that redshift range, so that the assumed $x_{\rm H\,I}$ should be regarded as an effective mean value, which includes such a variation (hereafter $x^{\rm eff}_{\rm H\,I}$).

TABLE 3

NIR AFTERGLOW INTRINSIC COLORS

Color	$\propto \nu^{-1/2}$	$\propto \nu^{-p/2}$ ($p = 2.5$)
I–*J*	0.70	1.0
I–*H*	1.3	1.9
I–*K*	2.0	2.8
I–*L*	3.1	4.3
J–*H*	0.62	0.86
J–*K*	1.3	2.8
J–*L*	2.4	3.3
H–*K*	0.67	0.91
H–*L*	1.8	2.4
K–*L*	1.1	1.5

NOTE.—In the observer's frame, the NIR afterglow spectrum of GRBs at $z \sim 10$ is proportional to $\nu^{-1/2}$ between $\sim$1 minute and several hours after the initial burst and proportional to $\nu^{-p/2}$ for later times.

[5] All magnitudes in this paper are in the Vega system.

In Figure 3, we show Δm_i for the I, J, H, and K bands as a function of the source redshift. The continuum in the observer's L band is not absorbed at all by the IGM neutral hydrogen when the source redshift is less than about 25. Although we assumed that the spectral shape is proportional to $\nu^{-1/2}$ in the panels, the results are much robust for the change of the spectral shape as noted above. The solid curves in these panels are loci of Δm_i for a given $x_{\rm H\,I}^{\rm eff}$ as a function of the source redshift z_S. For example, since $z^I_{{\rm Ly}\alpha,{\rm in}} = 5$ for I band, the IGM absorption in I band is about 5 mag for the source at $z_S = 7$ if the effective neutral fraction $x_{\rm H\,I}^{\rm eff}$ in the redshift range $5 \le z \le 7$ is 10^{-5}.

Two dotted vertical lines in each panel of Figure 3 indicate the redshifts when the Lyα break enters and goes out of each bandwidth ($z^i_{{\rm Ly}\alpha,{\rm in}}$ and $z^i_{{\rm Ly}\alpha,{\rm out}}$, respectively). As seen in Figure 1, if the IGM is significantly neutral, the source with $z_S > z^i_{{\rm Ly}\alpha,{\rm out}}$ cannot be detected through the filter i (i.e., *dropout*). However, we can detect such a source if the universe is highly ionized, since the continuum below the Lyα break remains as shown in Figure 2.

Suppose we observe a source with $z_S > z^i_{{\rm Ly}\alpha,{\rm out}}$ through the i and j filters and assume that the radiation through the j filter is not affected by any intervening absorption (i.e., $\Delta m_j = 0$). From equation (12), the expected magnitude through the i filter is

$$m_i = m_j + (m_i - m_j)^{\rm int} + \Delta m_i. \qquad (14)$$

For example, we consider the case of $i = I$, $j = L$, and $z_S = 7$. We find that the apparent L magnitude of the afterglow of a GRB at $z_S = 7$ for 1 hr after the prompt burst is about 14 mag from Figure 4. Thus, the apparent I magnitude is expected to be 22 mag because the intrinsic $I - L = 3.1$ mag for 1 hr (i.e., the case $\propto \nu^{-1/2}$ in Table 3) and $\Delta I \sim 5$ mag if $x_{\rm H\,I}^{\rm eff} = 10^{-5}$ in the redshift range $5 \le z \le 7$. We can reach 5 σ detection of the source with $I = 22$ mag by only 3 minutes exposure with a 8 m class telescope. Interestingly, the assumed $x_{\rm H\,I}^{\rm eff}$ is similar to the value reported by White et al. (2003) from the Gunn-Peterson trough in spectra of $z > 6$ quasars.

Similar arguments can be done for other bands. Therefore, in general, the detection of a source with $z_S > z^i_{{\rm Ly}\alpha,{\rm out}}$ in the filter i is the very good evidence that the universe in the redshift range $z^i_{{\rm Ly}\alpha,{\rm in}} \lesssim z \lesssim z_S$ is highly ionized, i.e., $x_{\rm H\,I}^{\rm eff} \ll 1$ in that redshift range. Conversely, the detection enables us to estimate $\tau_{\rm eff}$ and $x_{\rm H\,I}^{\rm eff}$. Finally, we note here that Figure 3 is also useful for other sources (e.g., QSOs), because Δm_i is almost independent of the source spectrum.

6. DISCUSSIONS

6.1. *Was the Universe Reionized Twice?*

Here we discuss how we can confirm or refute Cen's scenario, in which the universe was reionized twice. In this scenario, the first complete ionization at $z \sim 20$ is followed by the partially ionized epoch at $z \sim 10$. Therefore, we should check

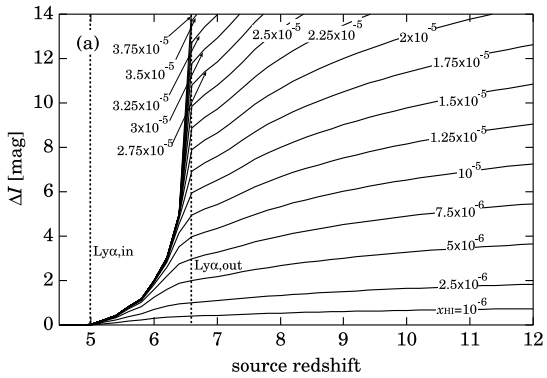

FIG. 3*a*

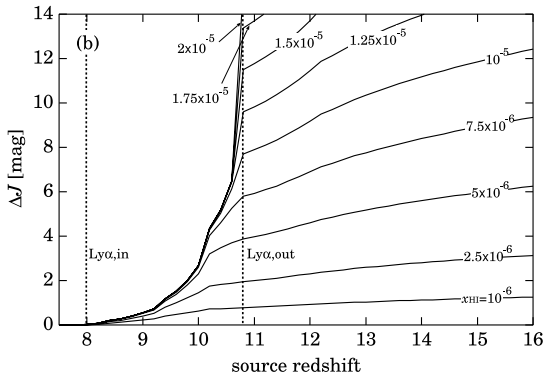

FIG. 3*b*

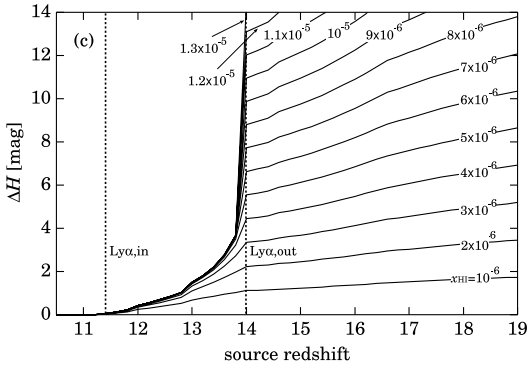

FIG. 3*c*

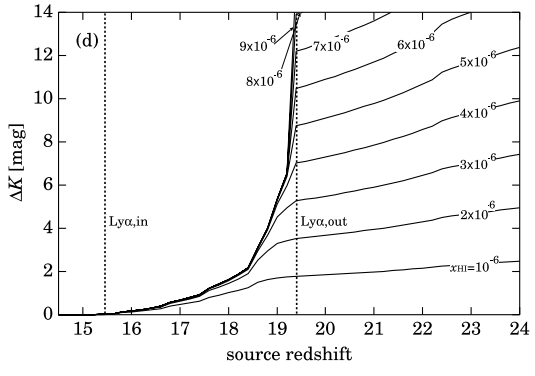

FIG. 3*d*

FIG. 3.—Intergalactic absorption in near-infrared bands. *Vertical axis*: Absorption amount in each filter (see eq. [11]): (*a*) I band, (*b*) J band, (*c*) H band, and (*d*) K band. *Solid curves*: Loci of the absorption amount as a function of the redshift of the source z_S. The neutral hydrogen fraction, $x_{\rm H\,I}$, is assumed to be constant between the redshift when the Lyα break enters the filter transmission and z_S. The assumed $x_{\rm H\,I}$ is indicated on each curve. Two dotted vertical straight lines in each panel indicate the source redshifts at which the Lyα break enters and goes out of the filter.

whether the neutral fraction at $z \sim 20$ is very low or not and whether the fraction at $z \sim 10$ is almost unity or not. To do so, the best observation is spectroscopy in the NIR bands. As shown in Figure 2, the reionization history is imprinted in the observed continuum. However, the sensitivity of the spectroscopy is in general much less than that of the photometric observations. Hence, we discuss the method using NIR photometry.

In § 5, we have shown that the detection of GRB afterglows through a filter i beyond the Lyα dropout redshift ($z^i_{\mathrm{Ly}\alpha,\mathrm{out}}$) proves the ionization of the universe around $z^i_{\mathrm{Ly}\alpha,\mathrm{out}}$. From the characteristic redshifts for the NIR filters summarized in Table 2, the I, J, H, and K filters are the most suitable to check the ionization state at $z \sim 5$–8, 8–11, 11–15, and 15–20, respectively. Thus, the null detection of the GRB afterglows of $z_S \sim 11$ in J band indicates a high neutral fraction in $8 \lesssim z \lesssim 11$. On the other hand, we detect the GRB afterglows of $z_S \sim 20$ in K band if the IGM in $15 \lesssim z \lesssim 20$ is ionized. The I- and H-band surveys are also very important to assess the reionization history of the universe. We can constrain the latest reionization epoch by observing GRB afterglows at $z \gtrsim 6$ in the I band. In summary, we can examine the reionization history by checking whether the high-z GRB afterglows drop out of the NIR filters or not.

In the rest of § 6.1, we discuss what is the difference between Cen's scenario and others. To demonstrate the main feature, we assume two schematic reionization histories: (1) single gradual reionization and (2) double sudden reionizations, which are shown in Figure 5 as the solid and dashed curves, respectively. These histories are based on two observational constraints: (1) the neutral fraction of hydrogen $x_{\mathrm{H\,I}} \sim 10^{-5}$ at $z \sim 6$ from the Gunn-Peterson trough found in the $z > 6$ quasars spectra (Becker et al. 2001; White et al. 2003), and (2) the beginning of the reionization is $z \sim 20$ from the large opacity of the electron scattering suggested by the *Wilkinson Microwave Anisotropy Probe* (*WMAP*) (Kogut et al. 2003). For the double reionizations, we also consider different values of $x_{\mathrm{H\,I}}$ in the first reionization epoch.

In Figure 6, we show the expected NIR colors as a function of source redshift for the afterglow spectrum $f_\nu \propto \nu^{-1/2}$ case (the observing time less than several hours; see Table 3). We find differences between single and double reionizations in the

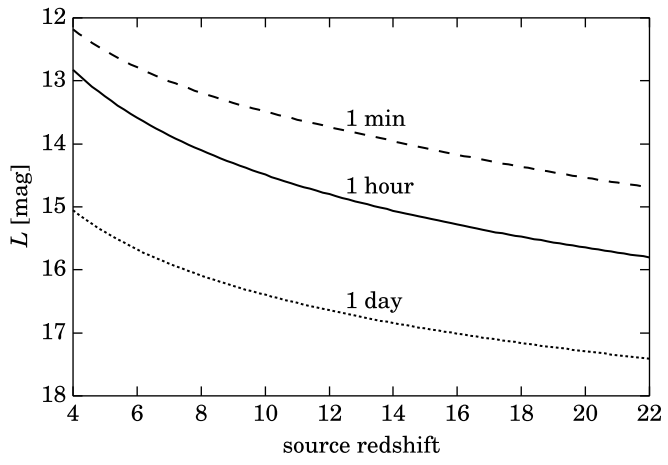

FIG. 4.—Expected apparent magnitude in L band of the afterglows of the gamma-ray bursts (GRBs) as a function of the source redshift. The dashed, solid, and dotted curves are the cases of 1 minute, 1 hr, and 1 day after the burst occurrence in the observer's frame, respectively. The spectral model of the GRB afterglows of Ciardi & Loeb (2000) is adopted. The assumed parameter set is described in the first paragraph of § 3.

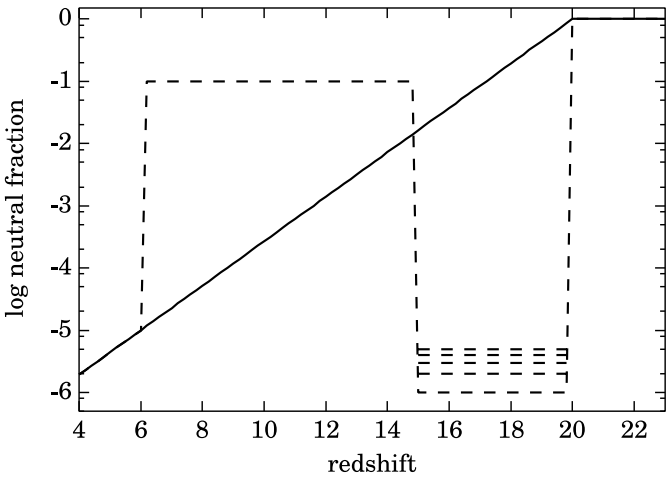

FIG. 5.—Examples of the reionization history. *Solid curve*: Single gradual reionization case. *Dashed curve*: Double reionizations case as suggested by Cen (2003a).

I–J (Fig. 6*a*) and K–L (Fig. 6*d*) colors. In Figure 6*a*, GRB afterglows up to $z_S \sim 8$ can be seen in both I and J bands for the single reionization case, whereas the I–J color of $z_S > 7.1$ afterglows diverges in the double reionization case, i.e., the sources drop out of the I band. This reflects the difference of the increasing rate of the neutral fraction around $z \sim 6$ in two reionization histories. The dropout redshift in the double reionization case is determined by $\lambda_\beta(1 + z_{S,\mathrm{drop}}) = \lambda_\alpha(1 + z_{\mathrm{reion}})$, where λ_α and λ_β are the rest-frame wavelength of the Lyα and Lyβ lines, and z_{reion} is the sudden reionization redshift (Haiman & Loeb 1999). In our case, $z_{\mathrm{reion}} = 6$. It is worth to noting that GRB afterglows beyond the dropout redshift of the I band ($z^I_{\mathrm{Ly}\alpha,\mathrm{out}} = 6.6$) can be seen through the filter in both reionization histories.

In Figure 6*d*, we find a significant difference between the two reionization scenarios. While afterglows beyond the dropout redshift of the K band drop out of the filter for the single reionization, we can see such afterglows in the twice-reionized universe. On the other hand, afterglows with $z_S > 23$ drop out of the K band even in the double reionization case because the Lyβ break goes out of the filter transmission width, i.e., $\lambda_\beta(1 + z_{S,\mathrm{drop}}) = \lambda^K_{\mathrm{max}}[= \lambda_\alpha(1 + z^K_{\mathrm{Ly}\alpha,\mathrm{out}})]$, where λ^K_{max} is the maximum wavelength of the K-band filter. We note here that $z_{\mathrm{reion}}(= 20) > z^K_{\mathrm{Ly}\alpha,\mathrm{out}}$ in this case, whereas $z_{\mathrm{reion}}(= 6) < z^I_{\mathrm{Ly}\alpha,\mathrm{out}}$ in the above case.

Any difference between single and double reionizations cannot be found in the J–H (Fig. 6*b*) and the H–K (Fig. 6*c*) colors because the neutral fractions in both cases are high enough ($\gtrsim 10^{-4}$) to extinguish the continuum blueward of the Lyα break completely. That is, GRB afterglows beyond the dropout redshift cannot be seen in the J and H bands for both reionization histories.

Let us summarize how to confirm or refute Cen's scenario: We can conclude that the universe was reionized twice if (1) GRB afterglows with $z_S > z^K_{\mathrm{Ly}\alpha,\mathrm{out}}$ are detected in the K band and (2) afterglows with $z_S > z^J_{\mathrm{Ly}\alpha,\mathrm{out}}$ or $z_S > z^H_{\mathrm{Ly}\alpha,\mathrm{out}}$ drop out of the J or H bands. However, null detection of the $z_S > z^K_{\mathrm{Ly}\alpha,\mathrm{out}}$ GRB afterglows in the K band does not reject Cen's scenario at once. The null detection only shows that the neutral fraction at $z \sim 20$ is larger than $\sim 10^{-5}$. In any case, deep and prompt K-band photometry of high-z GRB afterglows is useful to examine the ionization state at $z \sim 20$.

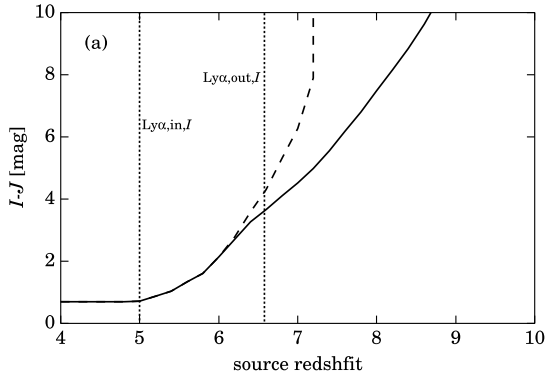

FIG. 6*a*

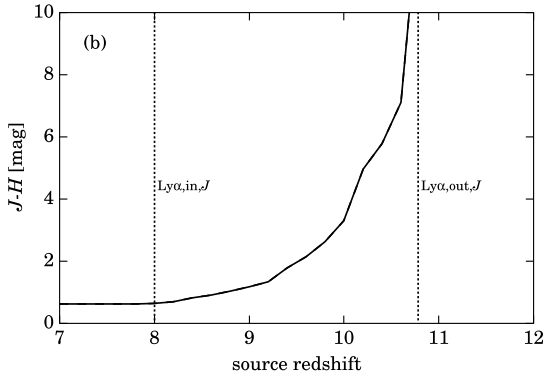

FIG. 6*b*

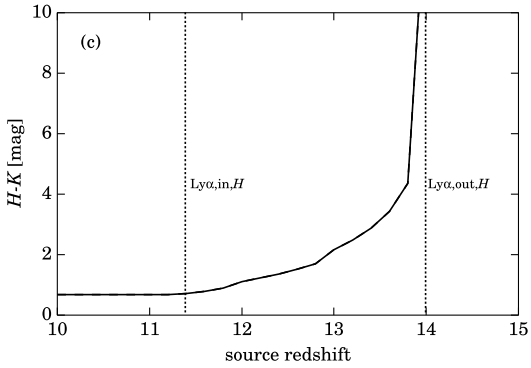

FIG. 6*c*

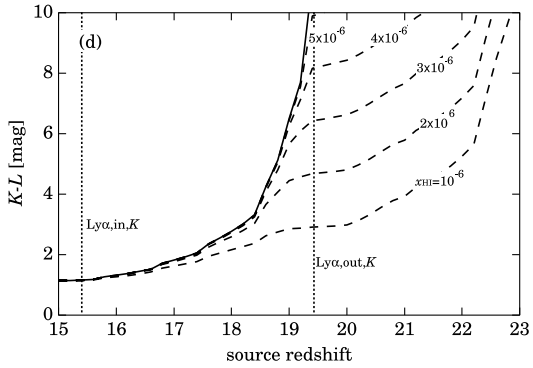

FIG. 6*d*

FIG. 6.—Expected near-infrared colors of gamma-ray burst afterglows. (*a*) $I-J$ colors, (*b*) $J-H$ colors, (*c*) $H-K$ colors, and (*d*) $K-L$ colors. The solid and dashed curves correspond to the cases of the single and double reionizations depicted in Fig. 5, respectively. The solid and dashed curves in (*b*) and (*c*) are perfectly superposed. In (*d*), some cases of the neutral hydrogen fraction in the first reionization are shown. Two dotted vertical straight lines in each panel indicate the source redshifts at which the Lyα break enters and goes out of the indicated filter.

6.2. *Comment on Lyman Break Technique*

In the above discussions, we assumed that GRB redshifts are known from other methods. Although spectroscopy of optical afterglows or host galaxies is used to determine the redshift of low-z GRBs, it may be difficult for high-z GRBs. The Fe line in the X-ray afterglow (Mészáros & Rees 2003) or some empirical method using the γ-ray data alone (e.g., Yonetoku et al. 2003) can be useful for the high-z GRBs. The search for the Lyα break is also useful. Indeed, spectroscopic detection of the sharp Lyα cutoff (see Figs. 2 and 3) is an accurate method to determine the redshift. However, the color-selection technique, which is often used to find $z \gtrsim 3$ galaxies (Madau 1995; Steidel et al. 1996), may not be good for high-z GRBs, since GRB afterglows beyond the dropout redshift of the considered filter can be detectable if the universe is sufficiently ionized.

For example, if we use $I - J \geq 5$ mag as a criterion to select high-z GRBs, the selected objects will have $z \gtrsim 6.5$ (see Fig. 3*a* and Table 3). However, a number of real $z \gtrsim 6.5$ objects escape the criterion if the neutral fraction is less than $\sim 10^{-5}$. Therefore, we cannot use a simple color-selection technique for high-z GRBs. Spectroscopic observations to detect the Lyα break feature or the Fe line (Mészáros & Rees 2003), or empirical methods using only the γ-ray data (Fenimore & Ramirez-Ruiz 2000; Norris et al. 2000; Ioka & Nakamura 2001; Amati et al. 2002; Atteia 2003; Murakami et al. 2003; Yonetoku et al. 2003) are required.

6.3. *Advantage and Disadvantage of NIR Colors Method*

The largest advantage of the NIR color method is that observations are easier and more sensitive than with other methods. The limiting magnitude with a high signal-to-noise ratio of broadband NIR photometry reaches much deeper than 20 mag in only a few minutes exposure with an 8 m class ground-based telescope. For example, the IRCS (Infrared Camera and Spectrograph) on the Subaru telescope (Japanese 8 m class telescope[6]) can reach the 2 σ upper limit of 22 mag in only 5 minutes exposure in K band. This magnitude corresponds to $\Delta K \simeq 5$ mag based on the expected L magnitude of $\simeq 16$ mag for the $z \simeq 20$ GRB afterglows at 1 hour after the burst (Fig. 4) and $K - L = 1.1$ (Table 3), and also corresponds to the neutral fraction of 3×10^{-6}. Thus, we can put this value as a lower limit of the neutral fraction at $z \sim 20$ for null detection.

A stricter lower limit can be obtained if we detect the emission from the reverse shock (Sari & Piran 1999a, 1999b; Gou et al. 2003). Some GRBs show a very bright early afterglow from the reverse shock. Interestingly, the apparent magnitude becomes $\sim$5–6 mag brighter than that shown in Figure 4. In this case, we can reach $\Delta K \simeq 10$, which corresponds to $x_{\rm H\,I} \simeq 6 \times 10^{-6}$. Very early observations are highly desired.

[6] See http://subarutelescope.org/.

From the detected magnitude or the limiting magnitude for the null detection, the neutral fraction or its lower limit in the corresponding redshift range can be estimated. However, the uncertainty of the neutral fraction obtained may be large if we have only one photometric datum, since the apparent dispersion of the afterglow luminosities is large. Even in that case, the uncertainty can be limited to a low level if we use more than two photometric data, i.e., colors, which are independent of the absolute luminosity. This point is one of the important advantages of the NIR color method. Therefore, NIR multicolor follow-ups of GRB afterglows are strongly encouraged.

Miralda-Escudé (1998) and Barkana & Loeb (2004) show that detailed spectroscopy of the red damping wing of the Lyα break provides us with the optical depth for the line, i.e., the neutral hydrogen column density to the source. However, the spectral resolution required is $\lambda/\Delta\lambda \sim 5000(10^5/\tau_{\mathrm{Ly}\alpha})$. For lower opacity, much higher resolving power is needed. The limiting magnitude for such observations becomes significantly shallower. That is, the method of damping wing measurement does not have sensitivity for a low-opacity case. On the other hand, the NIR colors method is sensitive for $\tau_{\mathrm{Ly}\alpha} \lesssim 10$. Therefore, these two methods are complementary to each other; if $x_{\mathrm{H\,I}} \sim 10^{-6}$ ($\tau_{\mathrm{Ly}\alpha} \sim 1$), the NIR colors method becomes very useful, whereas the damping wing method is promising when $x_{\mathrm{H\,I}} \sim 0.1$ ($\tau_{\mathrm{Ly}\alpha} \sim 10^5$).

Measurement of the CMB polarization anisotropy is also useful. Haiman & Holder (2003) show that we can distinguish how many times the universe was reionized by using EE spectrum with *Planck* sensitivity at the 3 σ level. Since the sensitivity of *WMAP* is not enough, we must await the launch of *Planck*[7] to reveal the reionization history through CMB measurements.

Moreover, metal absorption lines like O I λ1302 can be useful in determining the reionization history (Oh 2002; Furlanetto & Loeb 2003). However, the expected equivalent width is very small, $\lesssim$5 Å. We require spectroscopy with a resolving power $\sim$5000. Unfortunately, observations with a ground-based telescope may be difficult because many of Earth's atmospheric OH lines conceal the metal lines that are redshifted to the NIR. Only *JWST* (*James Webb Space Telescope*)[8] will have such a high spectral resolution among future space telescopes having NIR spectrographs. Thus, we need to await its launch to observe the metal absorption lines.

A technique using the hydrogen 21 cm absorption line has also been proposed (e.g., Madau et al. 1997). However, the brightness of GRB afterglows is too faint to use them as a background light source for present and future radio facilities, because the absorption line is very weak (Furlanetto & Loeb 2002). Thus, we need to look for other sources. Although Carilli et al. (2002) proposed luminous high-z radio-loud quasars as candidate background sources, it is very uncertain that they exist at $z \sim 20$.

The dispersion measure in GRB radio afterglows may be promising in the near future (Ioka 2003; Inoue 2003). If we observe the radio afterglow at about 100 MHz within about 1000 s after the burst occurrence, the delay of the arrival time of the low-frequency photons may be detectable by the Square Kilometer Array. Like the measurement of the red damping wing of the Lyα line, this technique is sensitive to $x_{\mathrm{H\,I}} \gtrsim 0.1$ (i.e., $\tau_{\mathrm{Ly}\alpha} \gtrsim 10^5$). Thus, this technique and our NIR color method also complement each other.

The disadvantage of the NIR color method is the coarse redshift resolution. As discussed in § 4, the neutral fraction obtained by the color method is averaged over in the redshift range of $z_{\mathrm{Ly}\alpha,\mathrm{in}} \le z \le z_S$. Thus, we cannot determine the so-called reionization redshift. Only the redshift range in which the reionization occurred is obtained. However, even such a rough redshift resolution is enough to show whether the universe was reionized once, twice, or more.

To know the detailed history of reionization, spectroscopy is needed. For this purpose, the Japanese astronomical satellite *ASTRO-F*[9] may be useful. The satellite will have a spectroscopic sensitivity of $\sim$30 μJy around $\sim$2 μm, which can detect GRB afterglows of $z_S \sim 20$ if $x_{\mathrm{H\,I}} \sim 10^{-6}$ (see Fig. 2*a*). *SIRTF* (*Space InfraRed Telescope Facility*)[10] may not be useful because it has such sensitivity only in wavelengths longer than 5 μm. In the future, *JWST* is very promising. Finally, we note that narrow-band photometry may be useful because its narrow transmission width provides us with a moderate redshift resolution while keeping a higher sensitivity than that of spectroscopy.

We thank Kunihito Ioka for valuable comments. This work is supported in part by Grants-in-Aid for Scientific Research of the Japanese Ministry of Education, Culture, Sports, Science, and Technology, 14047212 (T.N.) and 14204024 (T.N.), and also by a Grant-in-Aid for the 21st Century COE "Center for Diversity and Universality in Physics." A. K. I. and R. Y. thank the Research Fellowships of the Japan Society for the Promotion of Science for Young Scientists.

[7] See http://astro.estec.esa.nl/SA-general/Projects/Planck/.
[8] See http://ngst.gsfc.nasa.gov/.
[9] See http://koala.ir.isas.ac.jp/ASTRO-F/index-e.html.
[10] See http://sirtf.caltech.edu/.

REFERENCES

Amati, L., et al. 2002, A&A, 390, 81
Atteia, J.-L. 2003, A&A, 407, L1
Barkana, R., & Loeb, A. 2004, ApJ, in press (astro-ph/0305470)
Becker, R. H., et al. 2001, AJ, 122, 2850
Bessell, M. S. 1990, PASP, 102, 1181
Bessell, M. S., & Brett, J. M. 1988, PASP, 100, 1134
Bromm, V., & Loeb, A. 2002, ApJ, 575, 111
Carilli, C. L., Gnedin, N. Y., & Owen, F. 2002, ApJ, 577, 22
Cen, R. 2003a, ApJ, 591, 12
———. 2003b, ApJ, 591, L5
Chiu, W. A., Fan, X., & Ostriker, J. P. 2003, ApJ, 599, 759
Ciardi, B., Ferrara, A., & White, S. D. M. 2003, MNRAS, 344, L7
Ciardi, B., & Loeb, A. 2000, ApJ, 540, 687
Fenimore, E. E., & Ramirez-Ruiz, E. 2000, preprint (astro-ph/0004176)
Furlanetto, S. R., & Loeb, A. 2002, ApJ, 579, 1
Furlanetto, S. R., & Loeb, A. 2003, ApJ, 588, 18
Galama, T. J., et al. 1998, Nature, 395, 670
Giavalisco, M., et al. 2003, ApJ, in press (astro-ph/0309065)
Gou, L. J., Mészáros, P., Abel, T., & Zhang, B. 2003, ApJ, submitted (astro-ph/0307489)
Gunn, J. E., & Peterson, B. A. 1965, ApJ, 142, 1633
Haiman, Z., & Holder, G. P. 2003, ApJ, 595, 1
Haiman, Z., & Loeb, A. 1999, ApJ, 519, 479
Hjorth, J., et al., 2003, Nature, 423, 847
Inoue, S. 2003, MNRAS, in press (astro-ph/0309364)
Ioka, K. 2003, ApJ, 598, L79
Ioka, K., & Nakamura, T. 2001, ApJ, 554, L163
Kogut, A., et al. 2003, ApJS, 148, 161
Lamb, D. Q., & Reichart, D. E. 2000, ApJ, 536, 1
Leitherer, C., et al. 1999, ApJS, 123, 3

Loeb, A., & Barkana, R. 2001, ARA&A, 39, 19
Madau, P. 1995, ApJ, 441, 18
Madau, P., Meiksin, A., & Rees, M. J. 1997, ApJ, 475, 429
Matheson, T., et al. 2003, ApJ, 599, 394
Mészáros, P., & Rees, M. J. 2003, ApJ, 591, L91
Miralda-Escudé, J. 1998, ApJ, 501, 15
Murakami, T., Yonetoku, D., Izawa, H., & Ioka, K. 2003, PASJ, 55, L65
Nakamoto, T., Umemura, M., & Susa, H. 2001, MNRAS, 321, 593
Nakamura, F., & Umemura, M. 2001, ApJ, 548, 19
Norris, J. P., Marani, G. F., & Bonnell, J. T. 2000, ApJ, 534, 248
Oh, S. P. 2002, MNRAS, 336, 1021
Onken, C. A., & Miralda-Escudé, J. 2003, ApJ, submitted (astro-ph/0307184)
Osterbrock, D. E. 1989, Astrophysics of Gaseous Nebulae and Active Galactic Nuclei (Mill Valley: University Science Books)
Peebles, P. J. E. 1993, Principles of Physical Cosmology (Princeton: Princeton Univ. Press)
Price, P. A., et al. 2003, Nature, 423, 844
Sari, R., & Piran, T. 1999a, ApJ, 517, L109
Sari, R., & Piran, T. 1999b, ApJ, 520, 641
Sari, R., Piran, T., & Narayan, R. 1998, ApJ, 497, L17
Sokasian, A., Yoshida, N., Abel, T., Hernquist, L., & Springel, V. 2003, preprint (astro-ph/0307451)
Somerville, R. S., & Livio, M. 2003, ApJ, 593, 611
Spergel, D., et al. 2003, ApJS, 148, 175
Stanek, K. Z., et al. 2003, ApJ, 591, L17
Steidel, C. C., Giavalisco, M., Pettini, M., Dickinson, M., & Adelberger, K. L. 1996, ApJ, 462, L17
Uemura, M., et al. 2003, Nature, 423, 843
White, R. L., Becker, R. H., Fan, X., & Strauss, M. A. 2003, AJ, 126, 1
Wiese, W. L., Smith, M. W., & Glennon, B. M. 1966, Atomic Transition Probabilities, Vol. 1 (NSRDS-NBS 4; Washington: GPO)
Wyithe, J. S. B., & Loeb, A. 2003a, ApJ, 586, 693
———. 2003b, ApJ, 588, L69
Yonetoku, D., Murakami, T., Nakamura, T., Yamazaki, R., Inoue, A. K., & Ioka, K. 2003. ApJ, submitted (astro-ph/0309217)